Case Report

Metastatic canine cutaneous clear cell adnexal carcinoma: case report

Gustavo Silva Schiavi[1,2] (https://orcid.org/0009-0005-2894-2694), Lais Medrado do Nascimento[2] (https://orcid.org/0009-0007-8462-2497), Carine Vieira do Amaral[2] (https://orcid.org/0009-0007-3781-3418), Luana Lopes Patente[2] (https://orcid.org/0000-0003-1620-254X), Evelin da Silva Souza[3] (https://orcid.org/0009-0004-9263-797X), Sandy Lorena Pulecio-Santos[4] (https://orcid.org/0000-0002-0684-7435), Juliana Viegas de Assis[2,3] (https://orcid.org/0009-0006-6257-0270), Alex Junior Souza de Souza[1,2*] (https://orcid.org/0000-0001-6201-2777)

[1] Programa de Pós-graduação em Saúde Única, Universidade Santo Amaro (UNISA), São Paulo, SP, Brazil

[2] Clínica Veterinária UNISA, Universidade Santo Amaro (UNISA), São Paulo, SP, Brazil

[3] Curso de graduação em Medicina Veterinária, Universidade Santo Amaro (UNISA), São Paulo, SP, Brazil

[4] Programa de Pós-graduação em Patologia Experimental e Comparada, Faculdade de Medicina Veterinária e Zootecnia, Universidade de São Paulo (USP), São Paulo, SP, Brazil

[*]**Corresponding author:** souzajralex@gmail.com

Submitted: January 8th, 2026. Accepted: April 9th, 2026.

Abstract

Canine cutaneous clear cell adnexal carcinoma (CCCCAC) is a rare primary cutaneous adnexal neoplasm. Microscopically, CCCCAC is characterized by dermal and/or subcutaneous

lobules of pleomorphic polygonal to spindle-shaped cells with clear, glycogen-rich cytoplasm containing variably sized vacuoles with indistinct borders frequently associated with peripheral palisading, follicular papillary mesenchymal body-like structures, comedonecrosis, and lymphovascular invasion. Despite aggressive microscopic features, the biological behavior of CCCCAC in dogs remains poorly defined, and metastatic rates are likely underestimated. This report describes a metastatic case of CCCCAC in an 11-year-old mixed-breed, neutered male dog presenting with a cervical cutaneous mass and progressive pulmonary and lymph node metastases. Fine-needle aspiration cytology supported the diagnosis of a malignant epithelial neoplasm. Histopathology revealed a multilobulated, poorly demarcated, infiltrative neoplasm composed of clear cells with marked pleomorphism, high mitotic activity, comedonecrosis, and extensive lymphovascular invasion. Histochemical staining demonstrated cytoplasmic glycogen accumulation, as evidenced by periodic acid-Schiff positivity with diastase sensitivity. Immunohistochemically, neoplastic cells showed diffuse cytoplasmic immunoreactivity for pan-cytokeratin, variable expression of vimentin and S-100, and absence of melan-A, smooth muscle actin, and thyroid transcription factor-1 labeling, confirming the diagnosis of CCCCAC. Disease progression occurred despite supportive care, and necropsy revealed marked local aggressiveness and widespread metastases to lymph nodes, lungs, parietal pleura, and pancreas. To the authors' knowledge, this is the first documented case of metastatic CCCCAC in Brazil.

Keywords: dog, skin neoplasia, histopathology, immunohistochemistry.

Introduction

Clear cell adnexal carcinoma is a rare primary cutaneous adnexal neoplasm reported in humans (2–4,15) and dogs (1,5,8,12,14). In veterinary medicine, this entity has been described under several designations, including clear cell apocrine ductular carcinoma (6), clear cell

hidradenocarcinoma (7), follicular stem cell carcinoma (10,11), and, more recently, canine cutaneous clear cell adnexal carcinoma (CCCCAC) (1,5,8,9,14).

CCCCAC is an undifferentiated tumor. Although its histogenesis was initially attributed to apocrine glands (6), more recent histopathological, immunohistochemical (IHC), and ultrastructural findings support a follicular stem cell origin (5,8,9,12,14).

Microscopically, the neoplasm is located in the dermis and/or subcutis and is arranged in lobules of pleomorphic polygonal to spindle-shaped cells with abundant clear to vacuolated cytoplasm containing glycogen (5,8–10,12,14). Additional features variably observed and supportive of the diagnosis include peripheral palisading of neoplastic cells, multinucleation, spindle cells consistent with follicular papillary mesenchymal bodies, intracytoplasmic melanin, lymphovascular invasion, increased mitotic activity, and central lobular mineralization or necrosis (comedonecrosis) (5,6,8–10,14).

Despite the broad spectrum of cytomorphological changes, the predominance of clear cells guides the main differential diagnoses, including balloon cell melanoma, clear cell basal cell carcinoma, and sebaceous carcinoma (8–10,12,14,18). Histochemical stains such as periodic acid-Schiff (PAS), with and without diastase pretreatment, Fontana-Masson, and Oil Red O (in frozen sections) may assist in the diagnostic evaluation; however, particularly in poorly differentiated cases, definitive diagnosis relies on IHC. Neoplastic cells typically show coexpression of cytokeratin and vimentin, variable immunoreactivity for S-100 and melan-A, and lack immunolabeling for smooth muscle actin and calponin (8–10,12,14,18).

In humans, clear cell adnexal carcinoma predominantly affects men aged 50–70 years, occurs mainly in the head and neck region, and exhibits locally aggressive behavior with frequent post-excisional recurrence and metastasis to regional lymph nodes and lungs (2–4,16). In dogs, despite aggressive microscopic features, CCCCAC may show expansive or infiltrative growth and slow progression, favoring surgical excision (5,9,10,12,14). Although marked pleomorphism and frequent

lymphovascular invasion are commonly observed at diagnosis, reported recurrence and metastatic rates are low (10,14).

Given the limited number of documented cases, these rates are likely underestimated, underscoring the importance of appropriate clinical follow-up and systematic documentation of recurrent or metastatic lesions to better characterize biological behavior, prognostic factors, and potential breed- and sex-specific predispositions associated with CCCCAC (5,9,10,14). The present case report describes the anatomopathological and immunohistochemical features of a metastatic CCCCAC in a dog in Brazil.

Case description

An 11-year-old mixed-breed neutered male dog was presented with a 2-cm cutaneous mass in the right cervical region, with a one-month history and stable growth. Two months after initial evaluation, a second subcutaneous mass was detected ventral to the first lesion, adjacent to the right superficial cervical lymph node. This mass, which measured approximately 5 cm in diameter, was non-ulcerated, firm, and adhered to deep tissue planes.

Fine-needle aspiration cytology of both lesions revealed cohesive groups of epithelial cells with basophilic cytoplasm, increased nuclear-to-cytoplasmic ratio, coarse to reticular chromatin, mild anisokaryosis, and cytologic atypia, findings suggestive of an epithelial neoplasm. Thoracic radiographs revealed multiple nodular lesions within the pulmonary parenchyma, measuring up to 3.9 cm, consistent with metastases. Ultrasound-guided fine-needle aspiration of a pulmonary nodule revealed cells morphologically similar to those observed in the cervical cutaneous and subcutaneous lesions, but with more marked atypia, supporting the suggestive diagnosis of malignant epithelial neoplasia.

An excisional biopsy of the first cutaneous lesion in the right lateral cervical region was performed. Grossly, the lesion was a round, plaque-like, approximately 2-cm-diameter, pigmented,

alopecic mass with multifocal to coalescing ulceration (Fig. 1). On cut section, it was white, multilobulated, and fibroelastic. An incisional biopsy of the ventrolateral right cervical subcutaneous mass revealed similar gross features. Tissue samples were fixed in 10% neutral-buffered formalin, routinely processed, and stained with hematoxylin and eosin, periodic acid–Schiff (PAS), PAS with diastase pretreatment, and Fontana-Masson.

Immunohistochemistry (IHC) was performed on 4-µm sections mounted on silanized slides using antibodies against pan-cytokeratin (pan-CK; AE1/AE3), vimentin (V9), S-100, melan-A (A103), smooth muscle actin (SMA; 1A4), and thyroid transcription factor-1 (TTF-1), following appropriate antigen retrieval protocols (Table 1). Detection was achieved using a polymer-based system (Novolink polymer detection system, Leica biosystem) with 3,3′-diaminobenzidine as chromogen, and Harris hematoxylin counterstaining. Appropriate positive and negative controls were included.

Microscopically, the cutaneous mass was an exophytic and endophytic, highly cellular, poorly demarcated, multilobulated, non-encapsulated, and infiltrative neoplasm extending from the epidermis to the panniculus (Fig. 2A). Neoplastic cells were arranged in multiple lobules supported by a moderate fibrovascular stroma. Small aggregates of spindle cells resembling rudimentary follicular papillary mesenchymal bodies were observed. Peripheral palisading of neoplastic cells was frequent, while moderate to marked multifocal comedonecrosis was present within the centers of larger lobules.

Neoplastic cells were polygonal to spindle-shaped, with distinct cell borders and moderate to abundant clear cytoplasm, occasionally containing variably sized cytoplasmic vacuoles with indistinct borders (Fig. 2B). Nuclei were round to oval with finely stippled chromatin and one to two prominent nucleoli. There was marked anisocytosis, anisokaryosis, and pleomorphism, with occasional binucleation, 41 mitotic figures per 2.37 mm^2, rare atypical mitoses, and numerous lymphovascular invasion foci (Fig. 2C). Multifocal to coalescent intratumoral areas of moderate to

marked necrosis and hemorrhage were present, associated with a mixed inflammatory infiltrate composed predominantly of neutrophils and macrophages, with fewer lymphocytes and plasma cells.

Clear neoplastic cells showed mild cytoplasmic glycogen accumulation, predominantly at the tumor periphery, demonstrated by PAS positivity and diastase sensitivity (Fig. 2D). In a focally extensive area of overlying epidermal ulceration, discrete extracellular granular black pigment, more evident with Fontana–Masson staining, was interpreted as melanin pigment (pigmentary incontinence).

Immunohistochemically, neoplastic cells exhibited diffuse, moderate to marked cytoplasmic immunoreactivity for pan-CK (Fig. 3A). Vimentin expression was mild to marked in isolated clear cells (~5%) and strong and diffuse in the tumor stroma (Fig. 3B). S-100 immunoreactivity was multifocal and ranged from mild to marked in tumor cells (Fig. 3C). Melan-A expression was absent in neoplastic cells and restricted to residual melanocytes in the basal epidermis and hair follicles (Fig. 3D). SMA and TTF-1 immunolabeling were negative in tumor cells. Based on the histopathological and immunohistochemical findings, the diagnosis was CCCCAC.

The patient received supportive care, including topical wound management, analgesics, and corticosteroids for respiratory signs associated with pulmonary metastases. Approximately three months after biopsy, the non-excised ventral cervical mass exhibited rapid growth, inflammation, ulceration, and purulent exudation, accompanied by worsening hematologic and biochemical parameters and progression of pulmonary metastatic lesions on thoracic radiographs (Fig. 4). Four hundred and one days after initial presentation, the dog developed severe dyspnea and intense cervical pain, and euthanasia was elected. The carcass was submitted for necropsy.

Grossly, the right ventrolateral cervical region exhibited a focally extensive enlargement, forming a firm, erythematous mass approximately 10 cm in diameter, with a central, superficial, raised, ulcerated red area measuring approximately 1.5 cm (Fig. 5A). On dissection, the mass measured 10 × 7.5 × 10 cm, was white, multilobulated, poorly demarcated, and infiltrative, extending from the epidermis into the panniculus adiposus and deep muscle layers (including the

cleidocephalicus, longus capitis, and omotransversarius muscles), with proximity to major vessels and cervical vertebrae. An adjacent subcutaneous abscess (~5 cm) containing abundant purulent material communicated with the tumor surface through a fistulous tract.

Mandibular, superficial cervical, prescapular, axillary, and tracheobronchial lymph nodes were enlarged, white, and multilobulated on cut section (Fig. 5B). The lungs contained numerous multifocal to coalescing white nodules measuring 0.1–4.0 cm (Fig. 5C). The left caudal lung lobe was reduced in volume and contained a focally extensive, firm, non-crepitant, white multilobulated area involving approximately 60% of the lobe (Fig. 4D). Multifocal white nodules were also observed on the parietal pleura of the right hemithorax and within the pancreas.

Microscopically, the cervical tumor showed features consistent with the previously diagnosed CCCCAC, with numerous lobules of clear neoplastic cells extending from the epidermis into the subcutis and deep musculature (Fig. 6A). Compared with the original lesion, follicular papillary mesenchymal body–like structures were more frequent, and comedonecrosis was more pronounced. Neoplastic infiltration was observed adjacent to major cervical vessels, with perineural and periganglionic invasion, as well as involvement of the muscles surrounding the cervical vertebrae.

Metastatic lymph nodes showed complete effacement of the nodal architecture by variably sized lobules of neoplastic cells, separated by prominent desmoplastic stroma and exhibiting discrete to marked comedonecrosis (Fig. 6B). Similarly, most of the left caudal lung lobe parenchyma was replaced by metastatic CCCCAC arranged in lobules with marked desmoplasia and numerous foci of comedonecrosis (Fig. 6C). Metastatic lesions in the pulmonary parenchyma, parietal pleura, and pancreas were also confirmed (Fig. 6D), although desmoplasia was less prominent at these sites.

Discussion

CCCCAC is a rare primary cutaneous neoplasm, originally described in 1978 as clear cell hidradenocarcinoma (7). Because of the limited number of reported cases, its clinical presentation,

pathologic features, and biological behavior remain incompletely characterized (6,10,12–14,18). In this report, we describe the clinical findings and the gross, microscopic, histochemical, and immunohistochemical features of a metastatic case of CCCCAC.

CCCCAC predominantly affects older dogs and is generally characterized by a slow progression, even when lymphovascular invasion is present at diagnosis (10,14), as observed in the present case. There is no established consensus regarding clinical–surgical management or systemic therapy; however, surgical excision of the primary lesion with adequate margins, sometimes combined with regional lymphadenectomy, may result in prolonged survival, even in the absence of adjuvant chemotherapy (5,8). In this case, after excision of one cutaneous lesion and confirmation of pulmonary metastasis, supportive care was elected. Survival was 14 months after the onset of the first lesion, consistent with previous reports describing similar management (10,14). These findings highlight the importance of long-term follow-up to detect recurrence, metastasis, and to define prognostic factors better.

Fine-needle aspiration cytology was useful to confirm the epithelial and malignant nature of the cutaneous and pulmonary lesions; however, it was not diagnostic for CCCCAC. As previously reported, marked morphologic variability and the frequent absence of conspicuous glycogen vacuolization limit the diagnostic utility of cytology, reinforcing the need for histopathologic and immunohistochemical evaluation (12).

Microscopically, the cutaneous/subcutaneous and metastatic lesions supporting the diagnosis of CCCCAC were characterized by lobules of polygonal to spindle-shaped neoplastic cells with clear to vacuolated cytoplasm due to glycogen accumulation, confirmed by PAS positivity and diastase sensitivity, supported by a fibrovascular stroma. Additional features included peripheral palisading of neoplastic cells and structures consistent with rudimentary follicular papillae (7–10,12,14).

Historically, CCCCAC has been variably classified, initially compared with human clear cell hidradenocarcinoma with apocrine differentiation (7), later proposed as follicular stem cell carcinoma based on histogenesis (10,11), and subsequently debated due to the lack of specificity of glycogen

vacuolization and inconsistent follicular differentiation (15). As a result, alternative terms such as clear cell apocrine ductular carcinoma were proposed (6). However, later studies failed to identify consistent sebaceous, apocrine, or follicular differentiation and supported the current nomenclature CCCCAC, which was adopted in the present report (1,5,8,9,12,14,18).

Although clear to vacuolated cytoplasm is a hallmark of CCCCAC (8–10,14), this feature is not specific, as glycogen-rich clear cells may also be observed in the normal outer root sheath (ORS) and in several follicular neoplasms of dogs and cats, including trichoblastomas with ORS differentiation, inferior tricholemmoma, and granular trichoblastoma (8,9,17). In the present case, the diagnosis of malignancy was supported by the association of clear cytoplasm with adnexal differentiation features, marked cellular pleomorphism, anisocytosis and anisokaryosis, high mitotic index, necrosis, mineralization, and lymphovascular invasion, already evident in the initial biopsies, allowing exclusion of other follicular neoplasms (7–10,12,14,17).

The differential diagnosis included other clear cell neoplasms, such as balloon cell melanoma, clear cell basal cell carcinoma, sebaceous carcinoma, eccrine adenocarcinoma, and clear cell apocrine ductular carcinoma (5–9). Given the low degree of differentiation observed, these entities could only be excluded after integration of histopathologic, histochemical, and immunohistochemical findings (5,8).

In this case, the lobular architecture of clear cells with adnexal differentiation, the absence of melanin granules, diffuse immunolabeling for pan-cytokeratin (pan-CK), and the lack of Melan-A expression supported the exclusion of balloon cell melanoma, despite the reported variability of Melan-A expression in CCCCAC (8–10,14). Pan-CK expression, although nonspecific among epithelial tumors, represents an important diagnostic feature of CCCCAC (10,14,18).

Clear cell basal cell carcinoma was excluded based on the presence of pleomorphic spindle cells, multilobulated growth, predominantly vertical orientation, and aggressive metastatic behavior (5,8,9). Sebaceous carcinoma was considered unlikely due to the absence of basaloid reserve cells, residual sebocytes, or neoplastic cells with well-defined lipid vacuoles, even in the absence of lipid-

specific histochemical stains (5,8,9). Sweat gland neoplasms, including eccrine adenocarcinoma and clear cell apocrine ductular carcinoma, were excluded primarily based on lesion location and the absence of morphologic evidence of apocrine differentiation (5,8,9).

Vimentin expression in CCCCAC is highly variable (10,12,14); nevertheless, its coexpression with pan-CK, even when discrete, represents a relevant diagnostic feature and was observed in the present case (8–10,14). Multifocal S100 expression, also previously described in CCCCAC, was identified, although this marker is known to be highly variable and should be interpreted in conjunction with other antibodies and the clone used (10,12,14).

Although SMA expression has been interpreted as evidence of apocrine differentiation in isolated reports (13), the absence of morphologic apocrine features and negative SMA immunolabeling in this case support previous studies that use SMA negativity to exclude a myoepithelial histogenesis (10,12,14).

The metastatic behavior of canine CCCCAC remains poorly documented, largely due to the scarcity of necropsy-based studies (10,12,14). While regional lymph node metastases are relatively common, pulmonary and distant organ involvement is reported sporadically (10,12,14). In this case, prominent comedonecrosis and desmoplasia in nodal and pulmonary metastases, features previously described in CCCCAC, parallel those observed in human adnexal clear cell carcinoma with comedonecrosis (2–4). Negative TTF-1 immunolabeling further excluded a primary pulmonary epithelial neoplasm.

Necropsy findings demonstrated not only widespread metastatic dissemination, including lungs, parietal pleura, and pancreas, but also marked local aggressiveness, with infiltration of deep muscle planes, perineural and periganglionic invasion, and involvement of tissues adjacent to major vessels and cervical vertebrae, findings not previously reported (6–8,10,12,14). These observations emphasize the need for wide surgical excision with adequate margins and consideration of regional lymphadenectomy, particularly in tumors with high mitotic activity, as CCCCAC, although often described as slow-growing, may exhibit highly invasive and metastatic behavior (8).

To the authors' knowledge, this study represents the first documented case of metastatic CCCCAC in Brazil. The integrated characterization of clinical, gross, histopathological, histochemical, and immunohistochemical findings contributes to the morphological diagnosis of CCCCAC, broadens the understanding of its biological behavior and metastatic potential, and aids in the differential diagnosis of cutaneous clear cell neoplasms in dogs.

Data Availability

All the original contributions presented in this study are included in the article/supplementary material. Further inquiries can be directed to the corresponding author.

Author Contributions

Gustavo S. Schiavi: methodology, formal analysis, investigation, data curation, writing – original draft, and writing – review and editing. **Lais M. Nascimento**: formal analysis, investigation, data curation, writing – original draft, and writing – review and editing. **Carine V. Amaral**: methodology, validation, and investigation. **Luana L. Patente**: methodology, formal analysis, investigation, data curation, and writing – review and editing. **Evelin S. Souza**: methodology, formal analysis, investigation, data curation. **Sandy L. Pulecio-Santos**: methodology, formal analysis, investigation, data curation. **Juliana V. Assis**: supervision, methodology, formal analysis, investigation, data curation, writing – original draft, and writing – review and editing. **Alex J. S. de Souza**: conceptualization, supervision, methodology, formal analysis, investigation, data curation, writing – original draft, and writing – review and editing. All authors read and approved the final manuscript.

Conflict of Interest

The authors declare no competing interests.

Generative AI Use Statement

The authors did not use generative artificial intelligence tools or technologies in creating or editing any part of this manuscript.

Acknowledgments

The authors thank the professors and technical staff of the UNISA Veterinary Clinic who contributed to the clinical care of the animal and to the conduct of this study. The authors also thank the Laboratório de Patologia Diagnóstica e Ambiental, de Departamento de Patologia, Faculdade de Medicina Veterinária e Zootecnia, Universidade de São Paulo, which enabled the performance of part of the immunohistochemical assays.

Funding

The study was partially funded by Universidade Santo Amaro.

References

1. Bozkurt MF, Bhaya MN, Nişancı A. Cutaneous clear cell adnexal carcinoma in two dogs: cytological and immunohistochemical evaluation. *Ankara Univ Vet Fak Derg*. 2023;70(1):101-5. doi: 10.33988/auvfd.1102050.

2. Cazzato G, Bagaloni G, Sgarro N, Trilli I, Marzullo A, Giubellino A, Ribatti D. Malignant cutaneous clear cell tumours: a review of histological, immunohistochemical and molecular features. *Diagn Histopathol*. 2024;31(2):55-63. doi: 10.1016/j.mpdhp.2024.11.002.

3. Chaudhry IH, Zembowicz A. Adnexal clear cell carcinoma with comedonecrosis: clinicopathologic analysis of 12 cases. *Arch Pathol Lab Med*. 2007;131(11):1655-64. doi: 10.5858/2007-131-1655-ACCCWC.

4. Chén HZ, Jabin M, Tarbox M, Akin R, Sturgeon A. Adnexal clear cell carcinoma exhibiting comedonecrosis of the ear: a rare case treated with Mohs micrographic surgery. *Cureus*. 2024;16(7):e65041. doi:10.7759/cureus.65041.
5. Goldschmidt MH, Goldschmidt KH. Epithelial and melanocytic tumors of the skin. In: Meuten DJ, editor. *Tumors in Domestic Animals*. 5th ed. Hoboken: Wiley-Blackwell; 2017. p. 88-141.
6. Gross TL, Ihrke PJ, Walder EJ, Affolter VK. Sweat gland tumors. In: Gross TL, Ihrke PJ, Walder EJ, Affolter VK. *Skin Diseases of the Dog and Cat: Clinical and Histopathologic Diagnosis*. 2nd ed. Oxford: Blackwell Science; 2005. p. 665-94.
7. Jabara AG, Finnie JW. Four cases of clear-cell hidradenocarcinomas in the dog. *Aust Vet J.* 1978;54(9):420-3. doi: 10.1016/0021-9975(78)90006-3.
8. Kiupel M, editor. *Surgical pathology of tumors of domestic animals: epithelial tumors of the skin*. Vol. 1. Gurnee: Davis-Thompson DVM Foundation; 2018. 241 p.
9. Mauldin E, Welle MM. Integumentary system. In: Maxie MG (Ed). *Jubb, Kennedy, and Palmer's pathology of domestic animals*. 7th ed. St. Louis: Elsevier; 2025. p. 508-724.
10. Mikaelian I, Wong V. Follicular stem cell carcinoma: histologic, immunohistochemical, ultrastructural, and clinical characterization in 30 dogs. *Vet Pathol.* 2003;40(2):207-13. doi: 10.1354/vp.40-4-433.
11. Mikaelian I, Wong V. Letter to the editor. *Vet Pathol*, 2004;41:302. doi:10.1354/vp.41-3-302.
12. Piviani M, Sánchez MD, Patel RT. Cytologic features of clear cell adnexal carcinoma in 3 dogs. *Vet Clin Pathol.* 2012;41(1):127-31. doi:10.1111/j.1939-165X.2012.00434.x.
13. Sakuma A, Nishiyama S, Yasuno K, Ohmuro T, Kamiie J, Shirota K. A case of canine cutaneous clear cell adnexal carcinoma with prominent expression of smooth muscle actin. *J Toxicol Pathol*. 2010;23(4):265-269. doi:10.1293/tox.23.265.

14. Schulman FY, Lipscomb TP, Atkin TJ. Canine cutaneous clear cell adnexal carcinoma: histopathology, immunohistochemistry, and biologic behavior of 26 cases. *Vet Pathol.* 2005;42(2):111-122. doi:10.1177/104063870501700501.
15. Walder EJ. Letter to the editor. *Vet Pathol*. 2005;42:107-108. doi: 10.1354/vp.42-1-107-a.
16. Kazakov DV, Argenyi, ZB, Brenn T, Calonje E, Mehregan DA, Mehregan DR, Requena L, Sangüeza, OP, Santa Cruz DJ, Scolyer RA, Zembowicz A. Hidradenocarcinoma. In: Elder DE, Massi D, Scolyer RA, Willemze R (Eds). *WHO Classification of Skin Tumours*. 4th ed. Lyon: IARC; 2018. p. 164–165.
17. Wiener DJ. Histologic features of hair follicle neoplasms and cysts in dogs and cats: a diagnostic guide. *J Vet Diagn Invest.* 2021;33(3):479-497. doi:10.1177/1040638721993565.
18. Yasuno K, Nishiyama S, Suetsugu F, Ogihara K, Madarame H, Shirota K. Cutaneous clear cell adnexal carcinoma in a dog: special reference to cytokeratin expression. *J Vet Med Sci.* 2009;71(12):1609-1612. doi:10.1292/jvms.001513.

Table

Table 1. Antibodies, clones, manufacturers, dilutions, and antigen retrieval methods used in the immunohistochemical assays in a case of canine cutaneous clear cell adnexal carcinoma.

Antibody	Clone / Host / Type	Manufacturer	Dilution	Antigen Retrieval
Pan-cytokeratin (pan-CK)	AE1/AE3, mouse monoclonal (anti-human)	Dako	1:400	Citrate buffer, pH 6.0
Vimentin	V9, mouse monoclonal	Dako	1:100	Citrate buffer, pH 9.0
S100	Polyclonal, rabbit polyclonal	Dako	1:100	Citrate buffer, pH 6.0
Melan-A	A103, mouse monoclonal (anti-human)	Dako	Ready-to-use	EDTA buffer, pH 8.9
Smooth muscle actin (SMA)	1A4, mouse monoclonal (anti-human)	Dako	1:300	Citrate buffer, pH 9.0
Thyroid transcription factor-1 (TTF-1)	8G7G3/1, mouse monoclonal	Agilent Dako	Ready-to-use	EDTA buffer, pH 8.9

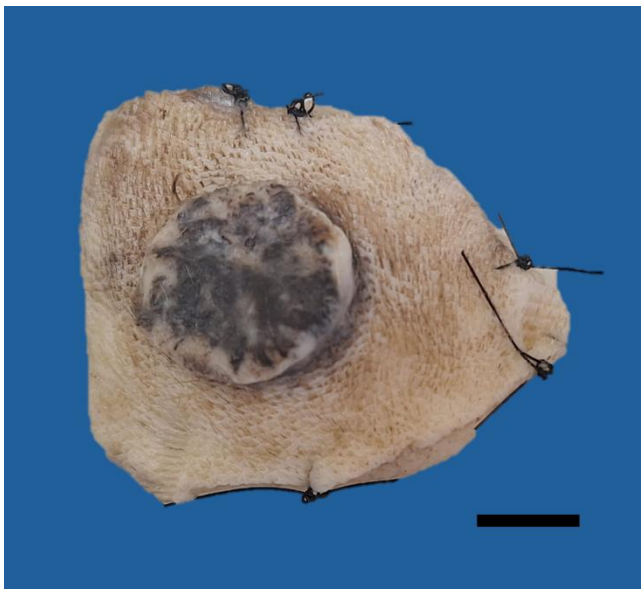

Figure 1. Canine cutaneous clear cell adnexal carcinoma, excisional biopsy (10% formalin-fixed specimen), dog. Note a round, plaque-like, alopecic, and pigmented lesion. Surgical sutures mark the margins. Bar = 1 cm.

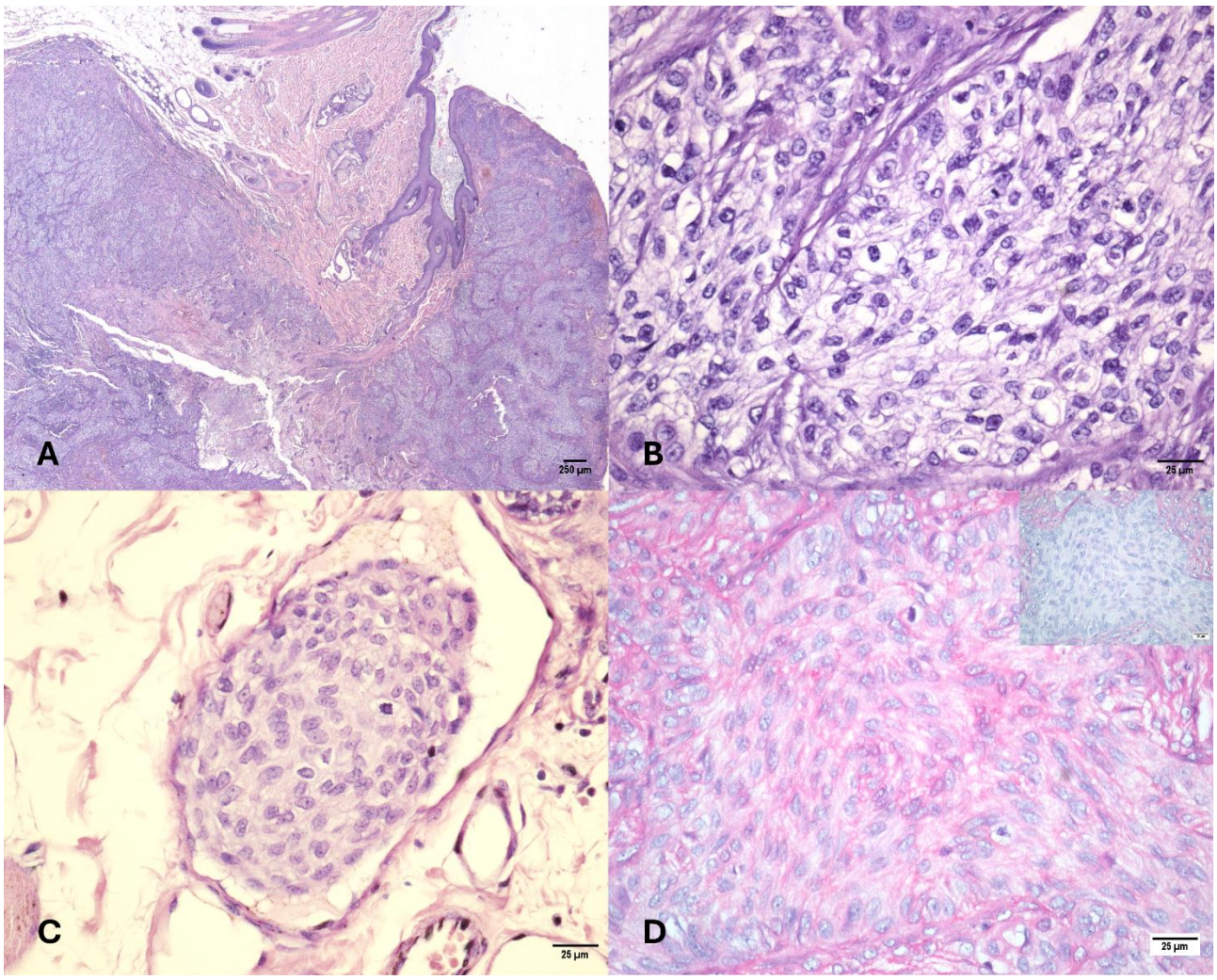

Figure 2. Canine cutaneous clear cell adnexal carcinoma, histopathology and histochemistry, skin, dog. A. Multilobulated clear cell neoplasm with exophytic and endophytic growth extending from the epidermis into the subcutis. Note a focally extensive area of central necrosis. H&E. Scale bar = 250 µm. B. Polygonal to spindle-shaped neoplastic cells with clear to vacuolated cytoplasm. H&E. Scale bar = 25 µm. C. Neoplastic embolus composed of clear cells. H&E. Scale bar = 25 µm. D. Lobule of clear cells showing discrete cytoplasmic glycogen accumulation. PAS. Scale bar = 25 µm. Inset: glycogen sensitive to diastase pretreatment. PAS with diastase. Scale bar = 25 µm.

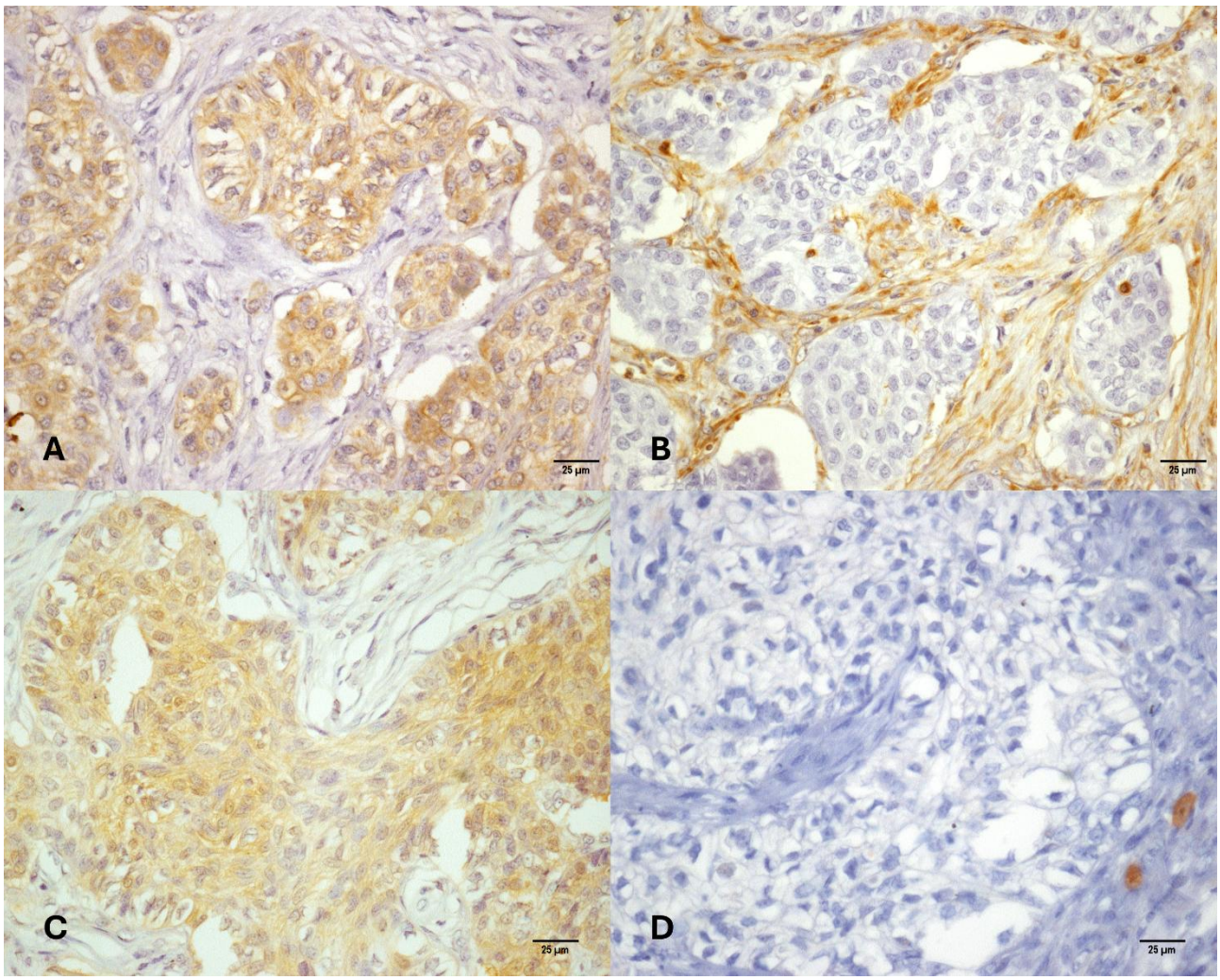

Figure 3. Canine cutaneous clear cell adnexal carcinoma, immunohistochemistry, skin, dog. A. Diffuse cytoplasmic expression of pan-cytokeratin (pan-CK) in neoplastic cells. Scale bar = 25 µm. B. Multifocal vimentin expression in isolated clear cells and diffuse immunolabeling of the tumor stroma. Scale bar = 25 µm. C. Positive S-100 immunolabeling in the cytoplasm of neoplastic cells. Scale bar = 25 µm. D. Negative Melan-A expression in clear cells and positive immunolabeling in two perifollicular melanocytes. Scale bar = 25 µm. Chromogen 3,3′-diaminobenzidine; counterstained with Harris hematoxylin.

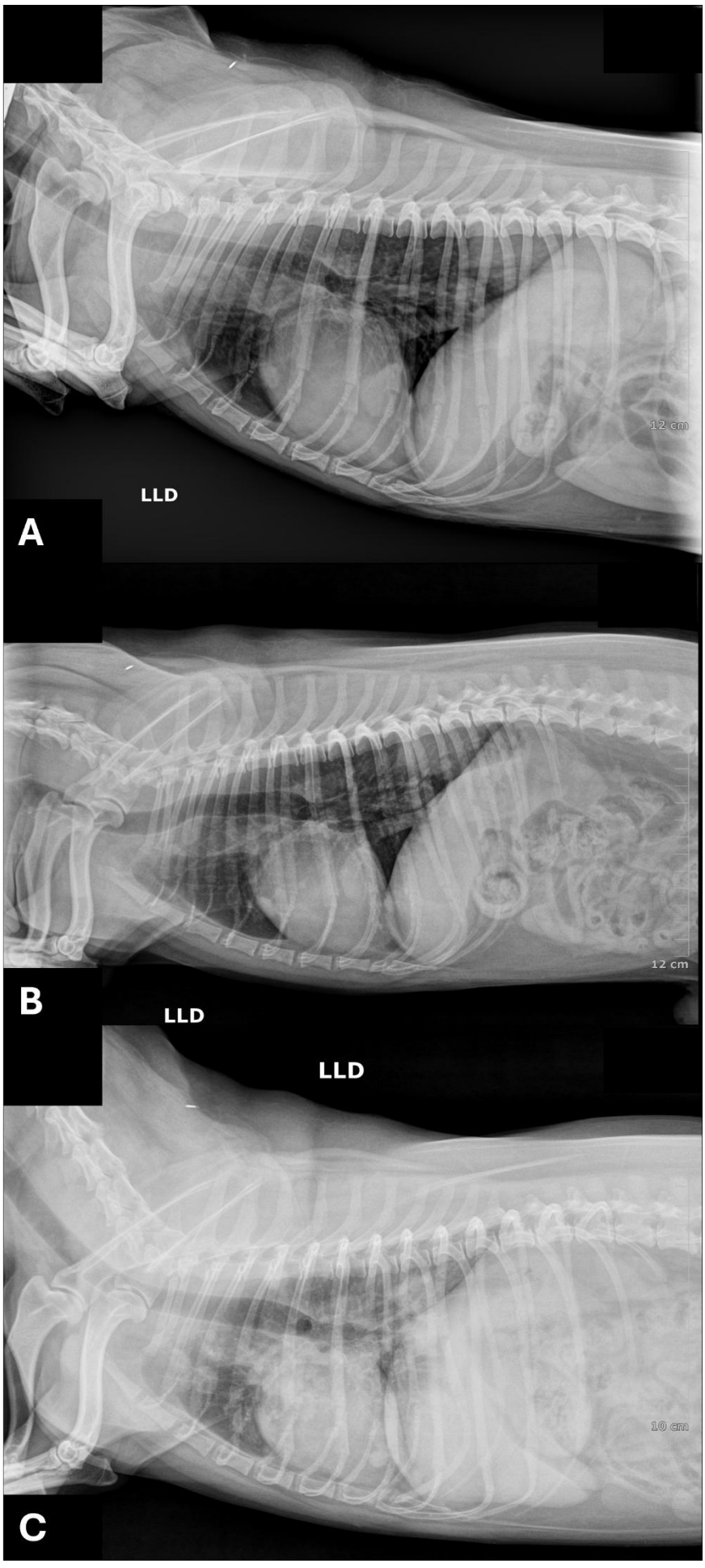
LLD
A
12 cm
B
LLD
LLD
12 cm
C
10 cm

Figure 4. Thoracic radiographs, dog. Note the progression of nodular structures with regular contours, homogeneous appearance, and soft-tissue (water) radiopacity, consistent with pulmonary metastases of canine cutaneous clear cell adnexal carcinoma. A. Thoracic radiograph at admission. B. Thoracic radiograph four months after admission. C. Thoracic radiograph nine months after admission. Legend: LLD = right lateral projection.

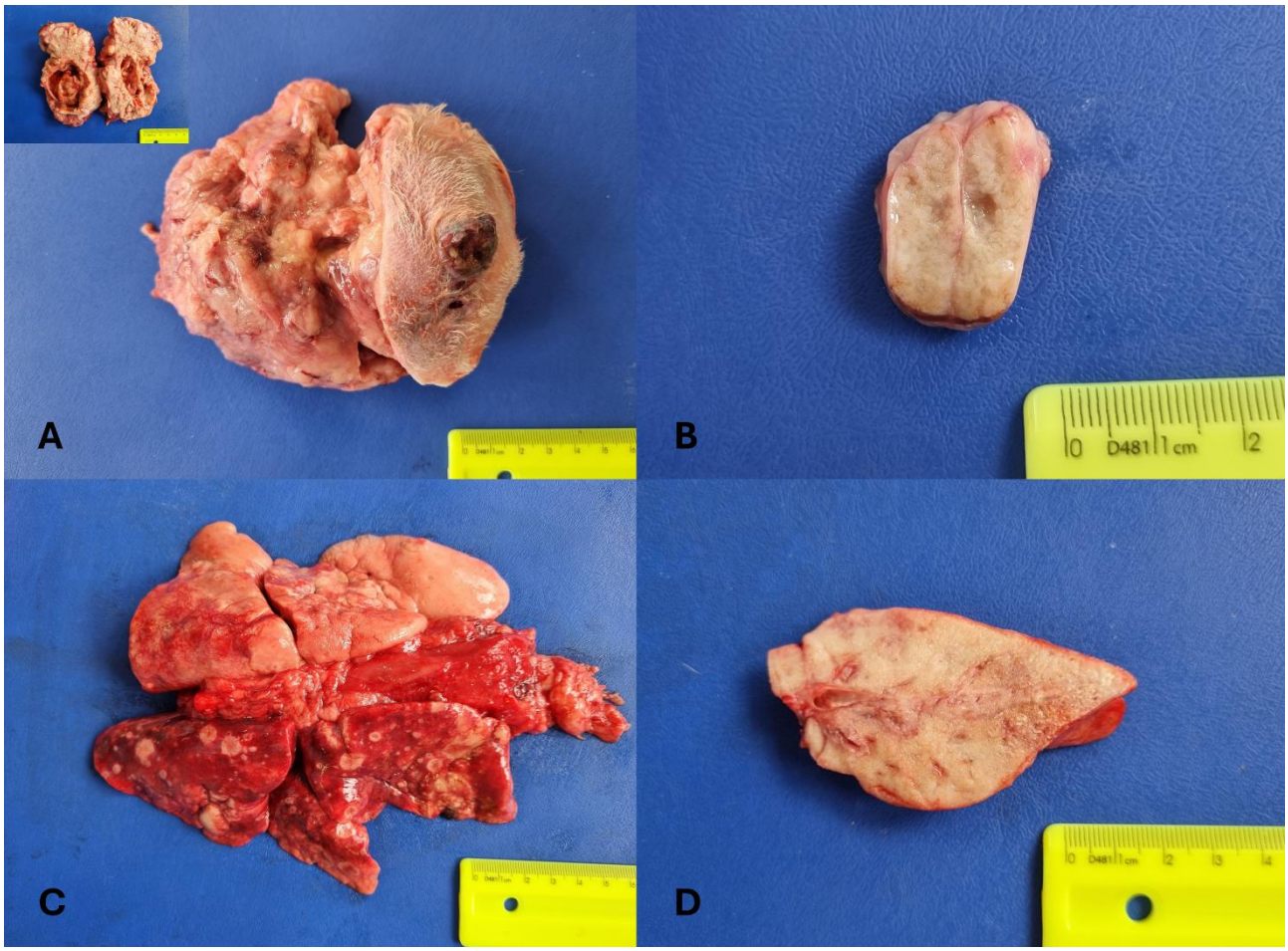

Figure 5. Canine cutaneous clear cell adnexal carcinoma, necropsy, dog. A. Neoplasm in the right ventrolateral cervical region after dissection. Note the centrally raised and ulcerated area. Inset: cut surface showing a multilobulated neoplasm extending from the epidermis into the subcutis; note an abscess adjacent to the tumor. B. Lymph node, cut surface. Note enlargement and a white, multilobulated parenchyma. C. Lungs. Randomly distributed, multifocal metastatic nodules and a focally extensive area of reduced volume in the left diaphragmatic lung lobe. D. Lung, cut surface of the left diaphragmatic lobe. Note the parenchyma completely effaced by a white, multilobulated mass.

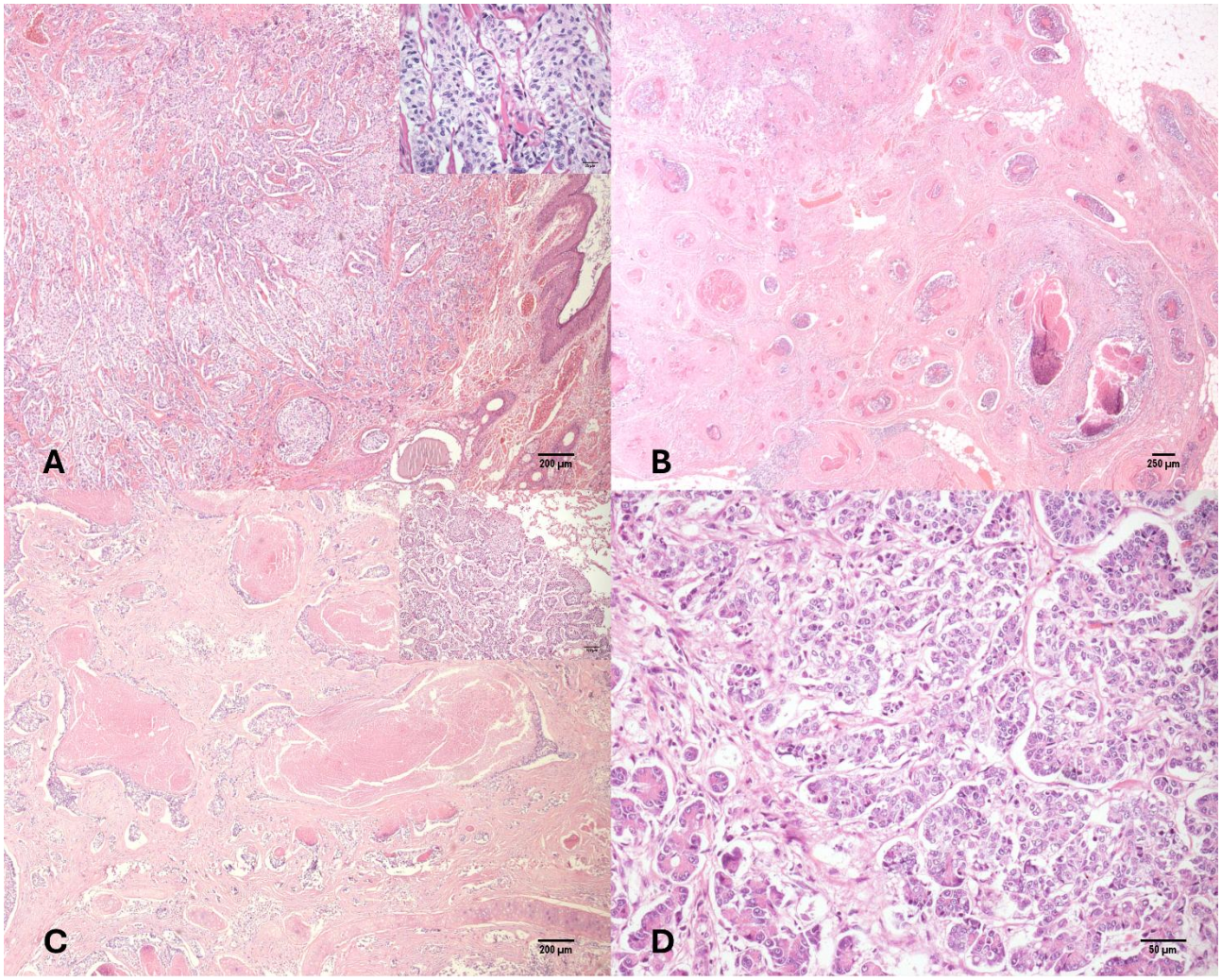

Figure 6. Canine cutaneous clear cell adnexal carcinoma, histopathology of tissues collected at necropsy, dog. A. Skin, clear cells arranged in lobules predominantly within the dermis. H&E. Scale bar = 200 µm. Inset: higher magnification highlighting clear cell detail. H&E. Scale bar = 25 µm. B. Lymph node, nodal parenchyma completely effaced by lobules of neoplastic cells with comedonecrosis, separated by marked desmoplastic stroma. Neoplastic infiltration of the perinodal adipose tissue is also present. H&E. Scale bar = 250 µm. C. Left lung (diaphragmatic lobe), parenchyma replaced by lobules of neoplastic cells with numerous areas of comedonecrosis, separated by prominent desmoplastic reaction. H&E. Scale bar = 200 µm. Inset: right lung, lobules of clear cells in a metastatic focus. H&E. Scale bar = 100 µm. D. Pancreas, metastatic clear cells within the exocrine pancreas. H&E. Scale bar = 50 µm.